Received: 9 September 2020 | Revised: 16 December 2020 | Accepted: 17 December 2020

DOI: 10.1002/eng2.12361

RESEARCH ARTICLE

WILEY

Facile engineering and interfacing of styrenic block copolymers devices for low-cost, multipurpose microfluidic applications

Hugo Salmon[1] | **M. Reza Rasouli**[1] | **Nicholas Distasio**[1] | **Maryam Tabrizian**[1,2]

[1]Biomedical Engineering Department-Faculty of Medicine, McGill University, Montreal, Quebec, Canada

[2]Faculty of Dentistry, McGill University, Montreal, Quebec, Canada

Correspondence
Maryam Tabrizian, Biomedical Engineering Department-Faculty of Medicine, McGill University, Montreal, Quebec, Canada.
Email: maryam.tabrizian@mcgill.ca

Funding information
Natural Science and Engineering Research Council of Canada, Grant/Award Number: RGPIN-2016-05785; Discovery and Strategic Grant, Grant/Award Number: STPGP 521532-18

Abstract

Soft thermoplastic elastomers (sTPE) and specifically styrenic block copolymers (SBC) are making rapid progress in the prototyping and mass production of microfluidic chips. However, these new materials lack guidelines and protocols for chips fabrication, curbing their widespread applications compared to polydimethylsiloxane. In this work, the prototyping potential of a commercially available SBC material, Flexdym, for continuous flow applications is explored. This SBC material exhibits both reversible and permanent self-adhesion depending on the time and bonding temperature, allowing for rapid and adaptive chip fabrication. Replicates are embossed in 2 min, assembled and sealed in 10 min. Under continuous flow, stud interfaces fabricated with this method can withstand 1 bar with reversible bonding and up to 3 bar after permanent bonding. The integration of an acoustic transducer in an SBC chip to induce acoustic streaming enables rapid mixing and local enrichment of polystyrene microparticles up to 8× the injected concentration. The reversible bonding feature of SBC chips allows to culture endothelial cells in open channels and then close and perfuse through channel to stain the cell. Our finding suggests that TPE-based materials offer numerous possibilities for prototyping microfluidic chips for analytical and biomedical applications when working with continuous flow at high pressure is required.

KEYWORDS

acoustofluidics, continuous flow, hot-embossing, open cell culture, soft thermoplastic microfluidics, styrenic block copolymer

1 | INTRODUCTION

From the roots of microelectronics fabrication, research on microfluidics devices started growing in cleanroom facilities offering the promise of transformative analytical tools, particularly in the life sciences. The choice of material based on physical, chemical and biological requirements and conditions of the intended experiment is the primary step in fabrication (of microfluidic devices). The most used materials so far, is polydimethylsiloxane (PDMS), a silicon oil-based biocompatible material widely used as a result of its ease of prototyping and high replication resolution.

However, the inherent limitations of PDMS including evaporation,[1] absorption,[2] leaching of uncrosslinked oligomers,[3] and surface regeneration due to hydrophobic recovery, were quickly surfaced.[4] In addition, the cost of the PDMS bulk oil (50 – 200 $/kg) as well as the equipment necessary for prototyping and mass production, curb its use for large-scale microfluidic chip prodcution.

To overcome inherent shortcomings of PDMS, the bio-inertness, biocompatibility, accessibility, and cost of any new materials must be considered for chip manufacturing, particularly for biological applications.[5-8] In the last decade, a considerable effort has been dedicated to developing microfluidic devices made of hard thermoplastics such as polystyrene (PS) and Cyclic Olefin Copolymer (COC) to bridge microfluidics and life sciences.[9-14] These polymers can be machined to make devices in few minutes in best configuration by computer numerical control machining,[15] industrial hot embossing,[16,17] or injection molding,[18] without taking into account the long heating or cooling cycles. There are now commercially available microfluidic platforms fabricated with these polymers. However, their fabrication requires expensive equipments and cannot be implemented in regular laboratory setting, reducing their widespread applicability.

Soft thermoplastic elastomers have thus emerged as a third generation of materials for chip fabrication due to their ease of prototyping, low cost, and biocompatibility (Table 1**)**. Examples of sTPE in biological applications include fluorinated ethylene propylene thermoplastic materials for immunoassay via covalent immobilization of antibodies,[26] thiol-ene-epoxy thermoset polymer resins on microarray surfaces,[27] and biocompatible and three-dimensional printable polyurethane-TPE filaments for valving and peristaltic pumping.[28] Particular efforts have been dedicated to developing microfabrication techniques for styrenic block copolymers (SBC), the price of which usually start as low as 10 $/kg for raw pellets. SBC are composed of styrene-ethylene-butylene-styrene, styrene-isoprene-styrene, and styrene-butadiene-styrene, presenting chemical similarities to PS.[29-33] The processing of soft SBC materials is also faster, less expensive, and simpler than "hard" TPE (2 – 5 GPa for COC and PS)[34] and though its development is not recent,[35] it keeps progressing particularly to make prototyping accessible and more user-friendly. For instance, commercially available SBC polymers, such as Flexdym™ (Eden Microfluidics, France) which is an oil-free SBC, allow for out-of-clean-room rapid prototyping. These materials are categorized as class VI USP in biocompatibility, making them suitable for chip device manufacturing for biological applications. In addition, the reduced manufacturing costs and know-how requirements that typically hinder the large-scale applicability of PDMS polymers make SBC soft materials an ideal candidate for microfluidic device scaled-up production. In lieu of a nanoprinter in a cleanroom, a recent study compared two approaches, nanoimprinting using a Nanonex and regular displacement based imprinting using a heat press, to emboss channels on Flexdym™ out of a mold made by lithography.[19] This embossing approach improved the fabrication speed and cost. However it lacked the ability to control the force over the applied pressure as the method was displacement-based, leading to high forces exerted on the mold and risk of breaking. A promising approach has recently emerged to use pressure-based systems such as the Sublym100 kit from Eden technologies, having already shown good prototyping compatibility with Poly(methy methacrylate) molds.[33] Though there exists a technical note to develop microfabrication out of styrene-ethylene-butylene-styrene co-polymer, there is a current lack of quantitative values and control the planarity, thickness of the embossed device. These requirements are critical for assembly and interfacing, particularly for multilevel devices, and to avoid deformation due to pressure on the channels (Table 2). Thus, there is not only a need for reproducible and robust techniques[36,37] to address prototyping limitations of microfluidic devices, but also simple, detailed, and cheap engineering methodology are required to ensure chip-to-world connectivity; a critical feature for microfluidic applications in analytical chemistry[38] as well as in life sciences.[39-41]

TABLE 1 Comparing properties of styrenic block copolymers (SBC) with thermoplastic elastomer in general (TPE), hard thermoplastics (TP), and polydimethylsiloxane (PDMS) materials properties for microfluidic technology

	SBC[19,20]	TPE[20-22]	TP[23,24]	PDMS[23,25]
Optical transparency	+++	++	+	+++
Young's Modulus	1–5 MPa	1–100 MPa	1–10 GPa	0.1–5 MPa
Molding	+++	++	+	+++
Gas permeability	Moderate	Moderate	Low	High
Cost ($/kg)	0.2–10	0.2–10	0.2–10	50–200
Reversible bonding	+++	+	Impossible	–
Irreversible bonding	+++	++	–	+
Demolding	++	++	–	+++

TABLE 2 Requirements and corresponding features for embossing styrenic block copolymers polymers

Requirement	Required features
Mold fidelity 	• deformation-free structures • burr-free channels • stable patterns
Transparency / optics 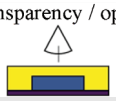	• dust-free surfaces • bubble-free device • mirror-like surfaces
Assembly / interfacing 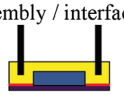	• planarity • mirror-like surfaces • pressure resistance

This study aims to develop out-of-the-cleanroom protocols using hot-embossing for fabricating robust and inexpensive chips out of an SBC material in less than 10 min that are suitable for reservoir-based, continuous flow, analytical chemistry, and cell culture applications. To this end, a methodology for the fabrication of such chips is described that includes parameters for embossing process, chip assembly, interfacing, and assessing chip performance for a variety of applications. Owing the low T_m of SBC material and its good capacity for flowing above T_m and merge in a single block in liquid phase, the hypothesis was that our hot embossing approach will allow to fabricate perfusable defect-free devices with control over chip planarity, thickness, and surface while obviating the need for precision tools for pressure and displacement monitoring as well as long thermal transition processes. Robust interfaces were made out of SBC pieces. Irreversible bonding performances as a function of time and temperature were assessed to confirm the intrinsic self-adhesion properties of the bulk material for robust interfacing. Reversible bonding was confirmed and repeated 10 times with similar pressure performances. The reservoirs were integrated into the chip to show the versatility of our approach to control the flow rate by hydrostatic pressure. The assembled device was also directly connected to a flow circuit to perform continuous flow experiments and evaluate the bonding robustness. An acoustic-based micromixer[42] was fabricated with hot-embossed SBC material and the capability of the devices for trapping and enrichment of microparticles based on their size was shown. The cell perfusion assay was also performed in the hot-embossed SBC microfluidic device by culturing primary mouse endothelial cells on the hydrophilized chip with open channels. The device was then reversibly closed, the cells were stained, and imaged using epifluorescence microscopy to verify the cell monolayer spreading and morphology in both open and perfused configurations.

2 | RESULTS AND DISCUSSION

2.1 | Development of a protocol for embossing of the sTPE devices

The embossing process and main parameters are described in Figure 1(A). The chips were fabricated using a sublimation oven adapted for embossing (Figure 1(B)), with a dedicated tray accommodating molds up to 6ε in diameter (Figure 1(C)). During phase (i) of embossing, the movement of the tray was governed by the pressure applied to the tray (0.4 – 0.7 bar) and the polymer flowing in its viscoelastic state (as $T = 150 - 170°C > T_m$). In phase (ii) the tray was blocked when it reached the spacers. To equally distribute the low pressure (0.4 – 0.7 bar) generated by vacuum, the top of the tray was covered by a silicon membrane. The temperature T was set above the material $T_m = 120\,°C$, from 150 ° C to 180°C, the upper temperature limit of the oven. The use of smooth silicon and metallic wafers allowed to fabricate even, reproducible, mirror-like surfaces and bubble-free replicas at 150 ° C in 30 s for simple channels (i.e., $100 \times 50\ \mu m^2$ cross section, covering a $25 \times 50\ mm^2$ microscope slide). The replication of mold structures on the embossed polymer was confirmed by profilometry—see Figure S3. While the pattern complexity was not critical for fabricating replicas above 1 μm, the replica quality was however highly dependent on the thickness of the sTPE as well as on the total embossed surface area. For the fabrication of devices with surface areas up to 100 cm^2 and thicknesses up to 3 mm at a temperature of 150 ° C, embossing time of 90 s was necessary (instead of 30 s).

The tray provided with the oven played a critical role in the final geometry of embossed devices. The tray had a 100 mm diameter groove to maintain the metal counter-mold horizontal during the process. The integration of spac-

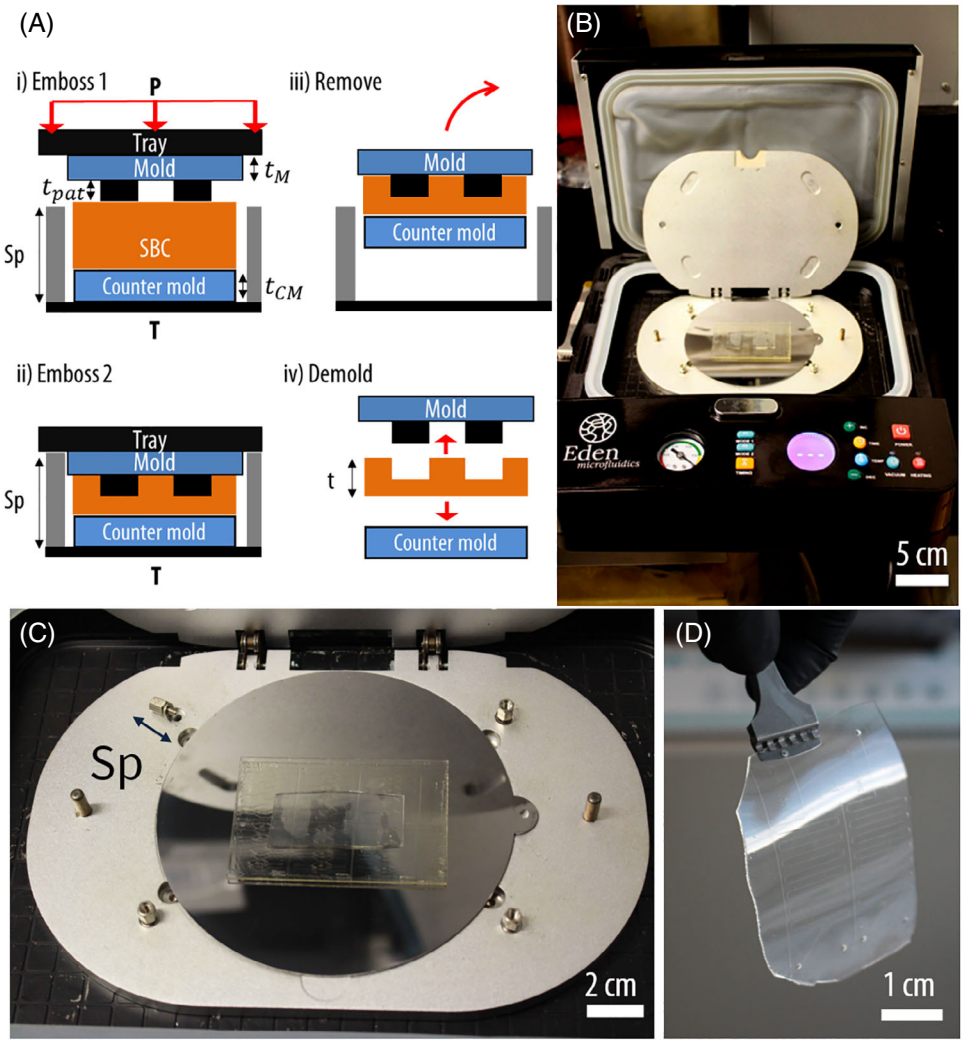

FIGURE 1 (A) Scheme of hot-embossing process with main microfabrication parameters (i–ii) embossing and (iii–iv) demolding. Overall thickness after embossing of the foil is *t*. (B) Top view of the sublimation oven used for isothermal embossing of microfluidic devices at $P = 0.7$ bar. (C) Top view of the tray, including a foil packed between a glass mold with microstructures of a thickness of "t_{pat}" and a metal counter mold. Spacers with a length of Sp are indicated by a black double arrow. (D) Picture of an styrenic block copolymers chip after embossing

ers and counter-molds in the embossing process (Figure 1(C)) also allowed to control the thickness and planarity of the embossed chip. Without these features, the embossing process stops at step (i) which leads to an uneven and usually thin embossed part. The surface of the counter-molds was smooth enough to fabricate the replica chip with high optical quality and sufficiently robust to undergo deformation without breaking during demolding. Although both metallic and silicon counter-molds could be used, metallic molds were better candidates than silicon wafers, as they were less prone to mechanical failure. For a metallic counter-mold combined with a 1 mm silicon mold, varying the size of the spacers (Sp) allowed for optimization of the chip's targeted thickness t, described as $t = Sp - 0.75 \pm 0.09$ mm in Figure S1. This relation which corresponds to the position where the tray is stopped by the spacers, can be generalized by the following Equation (1) $Sp = t_{CM} + t_M + t - 1.75$ mm where t_{CM}, t_M, and t are the thicknesses of the counter mold, mold, and the polymer replica after embossing, respectively. For the initial foil thickness condition (t_{foil}), we used $t_{foil} - H > 1.5t_{pat}$, where t_{pat} is the patterns maximum to allow for a sufficient amount of the melted SBC polymer to flow for bubble-free replication. The equilibrium was usually reached in less than 120 s, and it was possible to emboss replicates down-to ≈50 µm thickness without breaking the replicate. This embossing time was, however, longer when a greater volume of polymer and a higher space was used during embossing. Increasing the polymer volume helped for covering larger area and therefore more patterns but led to bubbles or burrs formation on the patterns. The cooling rate of the embossed stack was another factor to consider before demolding to avoid distortion and bubbles formation, and to respect the requirements as defined in Table 1.

The demolding step, that is, phases iii and iv, was particularly challenging due to the intrinsic adhesive properties of the sTPE material. This critical step could permanently damage both the sTPE foil and the micro/nano-mold.[43,44] As the polymer material and counter mold are hydrophobic, demolding becomes increasingly difficult with extending embossed surface area. To overcome this issue, isopropanol was sprayed on the polymer and counter mold as a lubricating layer

to facilitate the demolding of the embossed foil. Two approaches were tested in combination with lubrication: the use of SU8 primer layer or silane vapor deposition on the mold. The common approach consists in the deposition of the fluorine-based silane SU-8 layer to facilitate the first demolding. However, it compromises the uniformity and stability of silane layer, and contaminates the SBC chip with transfer fluorinated components (surveyed via XPS analysis, Figure S2), which leads to an undesirable nonuniform surface hydrophobicity. We thus tried a second approach by spinning a single primer layer of SU-8 photoresist epoxy resin before performing regular lithography. For medium size molds ($\approx$100 cm^2), this layer allowed for better adhesion of the structures to the wafer and resulted in long-lasting master molds. For designing chips larger than 100 cm^2, we found that a trade-off exists between the surface width and the adhesion of the mold. The combination of an SU-8 primer layer on the mold and a metal counter-mold allowed for safe demolding the chips. This approach also bypasses any chemical deposition or physical modification, leaving the pristine SU-8 as the surface of contact during the replication. For prototyping, the best combination was thus a primer layer of SU-8 on the mold, a thick metallic counter-mold and lubrication by isopropanol. Even recently, it was strongly suggested to use epoxy mold rather than a SU-8 master mold for high throughput production,[45] as it could make the mold more suitable for embossing. However, this change extended the device fabrication time. With the proposed demolding approach, the embossing process could be performed directly on the SU-8 master mold. The mold was made using regular optical lithography, which now can be performed out of clean room using UV LED maskers. This presents a significant advantage for rapid prototyping compared to the commonly used epoxy resin-based molds for hot-embossing. In addition, the silicon molds in this study, could be recycled more than 50 times without deterioration and the same metal counter-mold was employed for the fabrication of all chips. Through controlling the embossing parameters described above, high-quality SBC chips of precise thickness with flat mirror-like surfaces could be fabricated (Figure 1(D)), which were then used for further proof-of-concept studies as described in the following sections.

2.2 | Tailoring the embossed volume and recycling the polymer

As mentioned in previous sections, the initial volume of the foil to emboss is critical to properly mold the patterns. The overall initial thickness and surface coverage of SBC material to emboss was controlled by piling and properly aligning SBC chunks (Figure S4(A)). Embossing separated pieces of polymer, taking advantage of the inherent capacity of TPE polymers (and thus SBCs) to be remelted at a temperature above their T_m, can reduce significantly the polymer waste. As shown in Figure S4(A)–(C), the leftover chunks could be piled in a random manner, be remolded in a single block, be embossed to fabricate the chip in compliance with the requirements in Table 1. The raw SBC pellets (Figure S4(E)) could also be embossed for making the compliant chips (Figure S4(F)). SEM analysis of embossed surfaces fabricated from commercial unmodified SBC foils and from recycled chunks did not reveal any major difference between the polymer surfaces (Figure 2(A), (B)), the embossed patterns were burr-free and faithful to the master mold. The atomic force microscopy (AFM) images (Figure 2(C), (D)) of the patterns embossed on silicon confirmed that the embossing method did not induce any roughness artifact, the phase analysis confirming the typical amorphous long-chains network where the bright phase corresponds to PS and the dark phase to the rubbery matrix (i.e., ethylene-butylene, isoprene, butadiene) of SBC.[19] Fourier transform of the AFM phase distribution exhibited a 120 nm circular ring corresponding to a poorly ordered isotropic distribution which corroborates with the networks observed by AFM.[19] Thus, even though the polymer chunks have had a different thermal history, they could be embossed without further preparation to form a uniform block. The sTPE chunks were able to diffuse seamlessly at a temperature near the T_m (120 ° C) without applying any pressure (Figure S5). This recyclability of SBC materials provides an advantage over PDMS, since it reduces polymer cost and waste during the prototyping phase. Compared to other thermoplastics where the unused portions require a preliminary grinding step,[46] the recycling process here is simplified. Together, the capacity to tailor the embossing volume of SBC polymer as well as to recycle the polymer leftovers without any preprocessing, makes these polymers very coveted for scaled-up production as well as for prototyping, and the overall embossing methods could be adapted to other commercial SBCs.

2.3 | Interfacing of the chip and assessment of burst pressure

The self-adhesion properties of SBC allowed for the integration of microfabricated studs into the chips (Figure 3(A), (B)). To maximize the contact between the chip and its stud counterparts a subsequent curing step was performed to smoothen the surface and ensure the irreversible bonding.

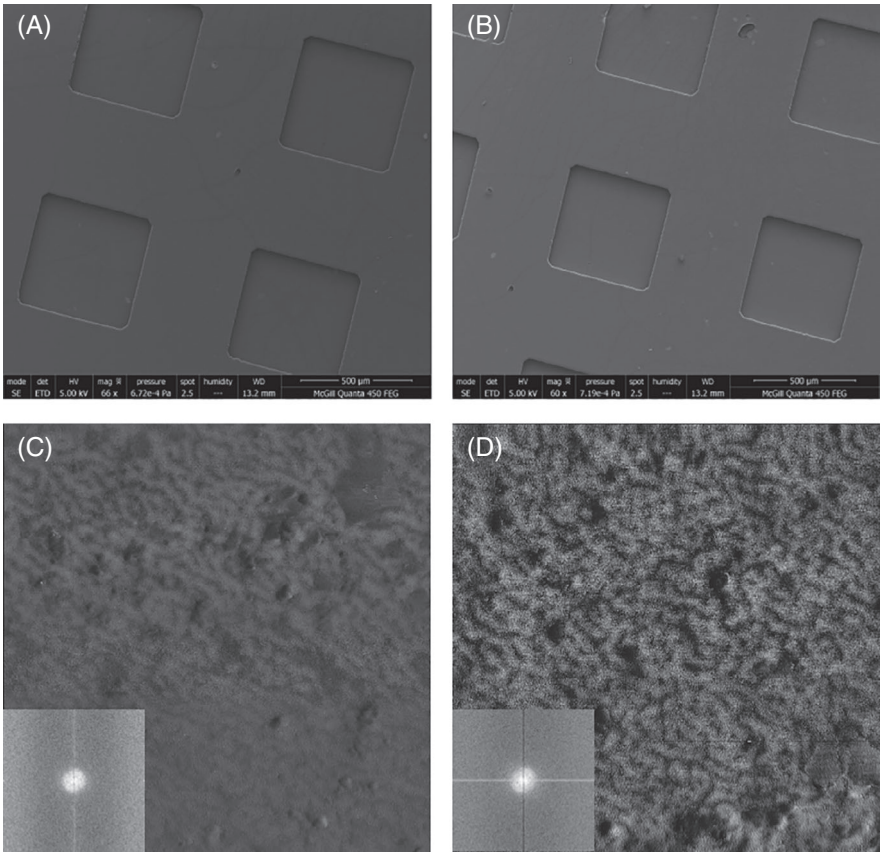

FIGURE 2 Representative SEM micrographs of embossed chip from (A) styrenic block copolymers (SBC) foil (B) recycled chunks of SBC; 0.9 × 0.9 μm AFM phase image and corresponding Fast Fourier Transform of (C) SBC foil (D) recycled SBC chunks

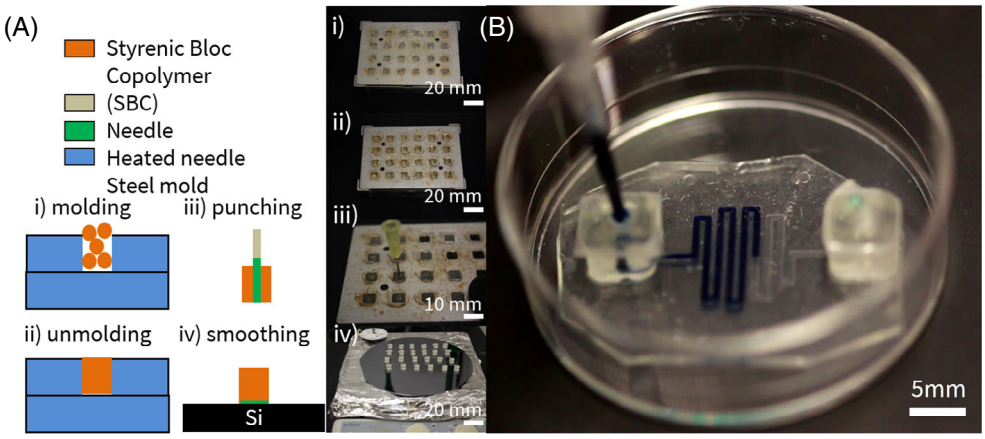

FIGURE 3 Chip interfacing by fabricating styrenic block copolymers (SBC) self-adhesive studs. (A) Microfabrication process flow of SBC stud interfaces and photographs for each step: (i) densely packing SBC pellets and molding, (ii) cooling down and unmolding, (iii) punching the stud with a heated needle, (iv) smoothening the stud bottom surface on a hot wafer (B) Chip interfaces were assembled allowing direct micropipetting

The chip was then used to determine, via burst pressure tests, the effect of contact time between two chip parts and temperature on the bonding strength. The burst pressure is done using a calibrated pressure controller and a tubing of negligible hydrodynamic resistivity. After 15 – min contact time at 80 ° C, the bonding was strong enough to break the chip parts before manually pulling off the studs. Further experiments confirmed that the strongest bonding occurred at 80°C for 15 – 30 min (Figure 4(A)). Leaving the chip at room temperature for 72 h also led to an equivalent bonding quality. As SBC is mainly composed of styrenic blocks, this temperature dependency of the bonding strength might be explained by the mobility of the free chains of the rubber matrix at the surface.[34] Though these chains are anchored to

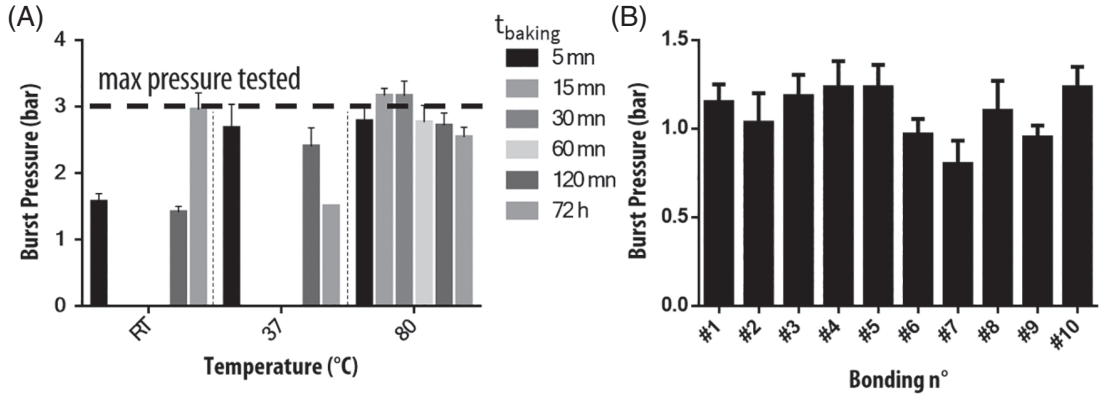

FIGURE 4 (A) Histogram displaying bonding strength as a function of the baking temperature and time. The horizontal dash line indicates the limitation of the pressure controller (3 bars). (B) Histogram displaying burst pressure as a function of the number of bonding/debonding cycles, repeated at room temperature for a t_{baking} of 15 mn. $n \geq 5$ chips for both tests

styrenic portions of the copolymer block, they are sufficiently long and mobile to induce intimate contact and thereby adhesiveness with the counterpart surface.[20,46,47] This leads to a reversible bonding that becomes sufficiently strong over time even below the melting temperature of the polymer (120 ° C). The increase of temperature from room temperature to 80°C accelerated the kinetics of diffusion without damaging the embossed fluidic structures as it was still below the melting temperature. Under optimal bonding conditions, no burst was observed even at 3 bar, the maximum pressure reachable by the pressure generator. This implies that SBC bonding would withstand even at higher pressure. The burst pressure always resulted in a leakage at the tube-stud junction and not in the channels. The Young's modulus of the SBC polymer is ≈1.15 MPa[19] in the same range as PDMS (0.5 – 3 MPa). Thus, a similar range of deformation of the chip is expected here as well at high pressure, which might lead to slight expansion (10% section increase at 3 bar for a 200 μm tape-sealed PDMS channel) of the channel section.[48,49] This bonding performance is similar to the bonding strategy for making sTPE-based chips using PCR tape[5] or gelatin-based adhesion.[8] Reversibility of chip sealing with a rinsing step was assessed using a T-shaped chip interfaced with studs. As illustrated in Figure 4(B), the strength of bonding remained above 1 bar even after 10 sealing/unsealing cycles and washing steps between each cycle. This result corroborates with the pressure values obtained at room temperature for short bonding time shown in Figure 4(A). The tolerance to high pressure makes SBC chips suitable for high pressure perfusion assays as well as for direct pipetting, a critical aspect in biologically based assays to minimize the use of reagents, and make the chips compatible with existing assays such as immunofluorescence. Overall, we provided a fully described and characterized method to mold stud interfaces out of SBC chunks that are inexpensive and simple to produce and provice a robust leak-free interface with better overall performances (>3 bar in best configuration) than what is currently described in the literature (2 bar in best configuration).[19]

2.4 | Passive perfusion assays using micropipette tip as reservoir

Pumpless microfluidics is of strong interest for many applications. Generally, for PDMS chips, reservoirs of various volumes are integrated during microfabrication process for performing pumpless liquid perfusion different flow rate. To demonstrate reservoirs can also easily be embedded in SBC-based chips in a tightly sealed manner, micropipette tips of various volumes (10, 100, and 1000 μL) were tested as reservoirs to confirm leak-free passive perfusion of liquid into the chip at different hydrostatic pressure (Figure S6(A)). After a 10 – min O_2 plasma hydrophilization of 25 – μm height channel networks, the passive perfusion of the liquid was confirmed by flowing via reservoirs and using micropipette tip, a diluted fluorescent rhodamine B solution. Thus, the reservoirs could easily be fitted without altering the good pressure performances of the bonding described in Section 2.3. Perfusion flow rate could be tuned as a function of the channel hydrodynamic resistance, allowing precise power-free control over flow. This is an interesting capability of SBC materials, as this principle can be used for example for emulsification of microdroplets in digital microfluidics.[50]

2.5 | Rapid micromixing and microparticle enrichment via integration of acoustic transducers into SBC devices

Piezo transducers used in bulk as well as boundary-driven micromixers are challenging to embed on-chip due to their size and the requirement for a physical proximity to the chip for transferring acoustic energy. We recently reported a state-of-the-art acoustic micromixer in PDMS chips where the integration of sharp edges with bubbles trapped between them, amplified the resonance phenomenon and generated fast and strong vortices for mixing.[42] The subsequent boundary-driven microstreams were then exerted to mix reagents for synthetizing nanoparticles with a narrow size distribution. However, the device channels had to be treated with parylene prior to nanoparticle synthesis to prevent leaching of unpolymerized PDMS oligomers. To take advantage of the rapid prototyping of SBC, an equivalent micromixer was fabricated by embossing a two-level mold (level 1: 100 μm, level 2:1 mm) to simultaneously pattern the transducer chamber and the fluidic circuit. The piezo element was then clamped to the substrate to generate acoustic waves within the channel. Its rectangular shape allowed to provide a closer proximity to the main channel than what was possible in our former paper.[42] The SBC chip was reversibly bonded to a glass substrate (Figure 5(A)) and our interfacing method allowed to perform continuous flow micromixing (Figure 5(B), (C) and Movie 3**)**. With a 4μl/min flow rate and a mixing length of 25.2 μm (Figure S7), a rapid mixing time of 7.2 ms was achieved. The transition regime, which was 150 ms, was obtained by alternating the acoustic transducer from ON and OFF while observing the fluorescence of the mixing zone (Figure S8). The mixing performance of the SBC-based device was comparable to its equivalent PDMS chip. As such, SBC materials could offer not only the possibility of rapid prototyping but also avoiding the issues of absorption, evaporation, and leaching associated with the use of PDMS.[23] The hydrophobic and gas-impermeable nature of the SBC even helped to stabilize the bubble trapped inside the sharp-edged compartments of the channel. In addition, the device could be sealed at room temperature to 80 ° C. This is an important consideration for fabrication of devices with embedded piezoelectric components as getting closer to their Curie temperature can affect the polarity, and thereby, their the piezoelectric properties.

The device was then used to trap and enrich fluorescently labeled latex microparticles of 3, 5, and 7 μm in diameter (Figure 6(A)**,** Movie 4**)**.[51] The local concentration is achieved using tracking—Movie 5. Once the particles were trapped, they could be released by simply switching off the acoustic field (Movie 6**)**. This ON/OFF cycle could be repeated until the desired enrichment was achieved. For example, a 10 μl sample of 5 μm beads suspended in water at a concentration of 10kparticles/ml could be locally enriched up to 8× the initial concentration (Figure 6(B)). To assess the local concentration of particles in the chip, N_{released} and N_0, corresponding to the numbers of particles tracked in a defined volume during the release phase and before trapping, respectively was measured and the enrichment factor, was determined using equation $\varepsilon = N_{\text{released}}/N_0$ (Movie 7**)**. The release of trapped particles can be achieved and controlled by generating acoustic waves below 100 kHz. This range of acoustic waves is close to the audible limit (20 kHz) thus constituting a limited cytotoxicity. Moreover, acoustic streaming used in this platform are shown to have minimal effect on the cell viability, proliferation and phenotypes.[52] This presents an advantage over the existing microparticle

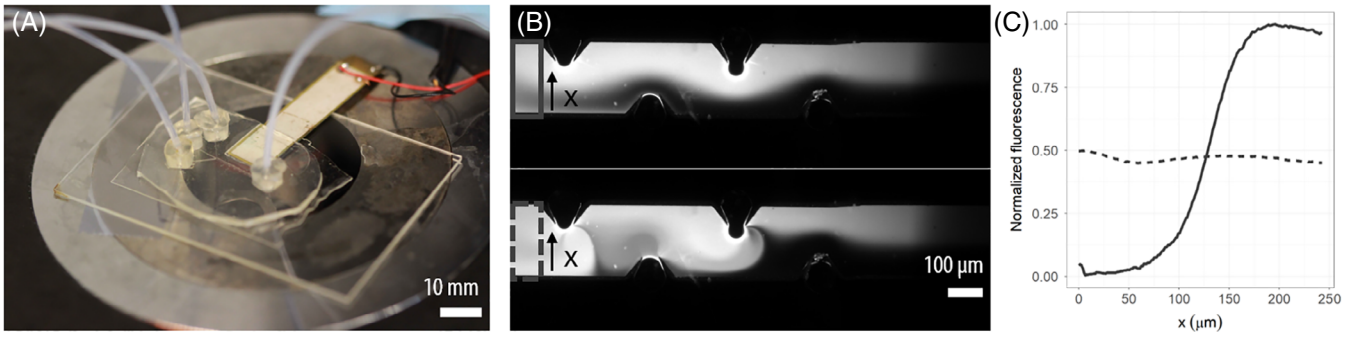

FIGURE 5 Integrated on chip bulk transducer and induced vortices in the main microchannel. (A) Photograph of a device embedding an acoustic transducer. (B) Micromixing of rhodamine B and buffered water generated by resonant solid–gas microstructures. Rectangular patterns indicate the measurement sections for nonmixing (solid line) and mixing (dash line) regions. (C) Normalized fluorescence comparison between a channel before (solid line) and after (dash line) mixing as a function of transverse position × in the channel

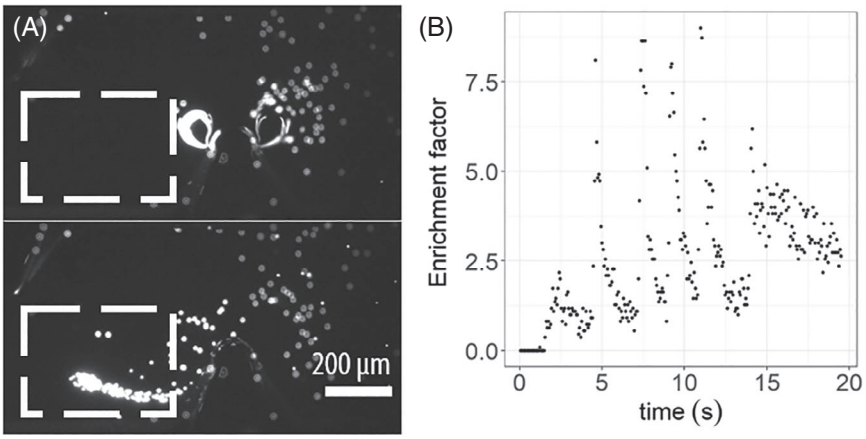

FIGURE 6 Microparticle sample enrichment using acoustic micromixer. (A) Enrichment of a 5.1 µm microparticle sample by resonant microstructures. The tracking is performed in the white rectangular area. (B) Factor of enrichment goes up to 8× and can be repeated several times. Particle counting in the defined rectangulars area based on Trackmate algorithm for enrichment

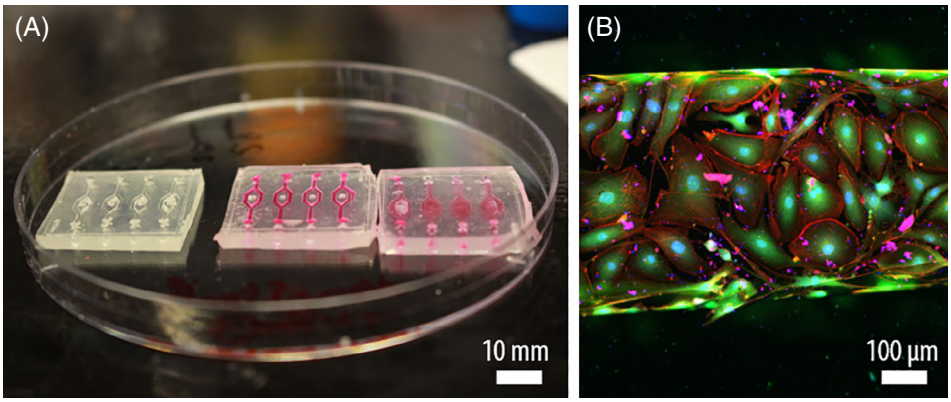

FIGURE 7 From open microfluidics to closed cell culture under flow. (A) Showing the open hydrophilized microchannels device, filled with 1 mM rhodamine B and then closed for perfusion assay. (B) Confocal microscope image of the grown endothelial cell monolayer stained with DAPI for nucleus (blue), GFP for cytoskeleton (green) and Phalloidin iFluor 594 for Actin fibers (red)

enrichment devices, as our SBC chip embedding an acoustic-based micromixer can be used with cells and micropollutants such as bacteria.

2.6 | Reversibly sealable device enables switching from open cell culture to perfusable devices

Selective hydrophilization of the channels by oxygen plasma (Figure S9) performed on temporarily closed chip by reversible bonding, resulted in a 30°-drop of the receding contact angle inside the channel (Figure S9(B),(C)). The channel hydrophilization allowed to guide and maintain liquids in the channels by capillarity forces (Figure S9(A)) for the following cell culture experiment with mECs, as hydrophilic surfaces are needed to ensure homogenous repartition of reagents in the channels. The confocal microscopy images of stained mECs after 24 h, which were cultured beforehand on gelatin coated open channels for 6 h (Figure 7(A)), confirmed the formation of a uniform and dense endothelial cell monolayer (Figure 7(B)). Although, the static culture of endothelial cells has previously been shown on SBC-based polymer Spinflex™,[19,30] this is the first demonstration of using SBC-based microfluidic chips for switchable open and closed cell culture. Such reconfigurable open microfluidics can facilitate chip assembly similar to polycarbonate (PC) chips[24] and offer the possibility of studying on-chip, the effect of various microenvironments on cells such as cell–drug and cell–particle interactions.[40,41] However, compared to PC material, our approach simplifies the chip prototyping. The embossed SBC chips are also well suited for investigating cells under flow shear stress. Furthermore, the ability to re-open the chips and have access to the cells could make this platform complementary with analytical techniques such as qPCR, western blotting, AFM, and flow cytometry.

3 | CONCLUSION

We described a new methodology for fabrication of SBC thermoplastics-based microfluidics as a value-added to the existing knowledge on this emerging material for microfabrication. The original interfacing techniques using hot-embossing allowed for assembly of robust SBC microfluidic chips in an easy, fast, and inexpensive manner, completing the existing knowledge around this emerging material. In less than an hour, fully interfaced SBC chips could be prototyped with integrated reservoirs and/or transducers for the rapid implementation of high-pressure continuous flow experiments such as microparticle enrichment or to be used as a platform for cell culture. The low temperature melting and adhesive properties of SBC material from the sTPE family, allowed for material recycling, and tailoring thickness of the final device during the fabrication process. In addition, taking advantages of the SBC thermal and viscoelastic properties, the proposed prototyping methodology allowed to emboss replicates in less than 2 min out of the clean-room facilities. This offers new avenues for prototyping analytical or biomicrofluidic solutions as well as forcommercialization of inexpensive kits to produce sealed microfluidic chips by simple heating. The embossed chips showed the capability of leak-free passive perfusion via pipetting and pipette-tip reservoirs as well as active perfusion by connection to a fluidic circuit. In the quest for a material that can offer easy and rapid prototyping and deliver high potential for industrial production, this work provides an original approach for the fabrication and integration of SBC chips as an enabling technology for a wide range of common microfluidic applications in particular for bioassays.

4 | EXPERIMENTAL SECTION

4.1 | Materials

Isopropanol and acetone were purchased from VWR. Negative photoresist (SU-8, 2015, 2050) and SU-8 developer were purchased from MicroChem Corp., USA. 1.1 mm Flexdym™ and polytetrafluoroethylene sheets, smoothened metallic wafer and Sublym 100 hot embosser were obtained from Eden Microfluidics (France). Rhodamine B and 4′,6-diamidino-2-phenylindole (DAPI) were purchased from Sigma-Aldrich. Phalloidin iFluor 594 was from Abcam (ab176757). Silicon wafers were purchased from University Wafer (USA). Inlets and outlets were punched using McGill Inc. hole punchers (USA). Fluorescein and trichloro(1H,1H,2H,2H-perfluoroctyl) silane were ordered from Sigma-Aldrich, Canada. 1 ml plastic Beckman–Dickinson syringes were purchased from Fisher Scientific, Canada. The piezoelectric transducer was a model SMBA4510T05M from Steiner Martins Inc., USA. Fluorescent PS particles (PSF-002U M) were purchased from Magsphere, USA. Tubing were 0.031×0.094 Tygon 3350 tubes from St Gobain, France.

4.2 | Mold fabrication

Mold fabrication required special care for adhesion and temperature resistance of the photoresist compared to standard MEMS microfabrication techniques due to the embossing temperature, which creates different thermodynamic conditions than other replica molding techniques used with PDMS. Silicon wafers (1 mm thickness 100 mm diameter) were dehydrated on a 150°C hot plate for 20 min to enhance adhesion of the photoresist to silicon. For stronger photoresist adhesion to the silicon, a thin first layer of 2015 SU-8 (below 10 μm) was coated on the wafer, flood-exposed, and post-baked. A second coating layer of 2015/2050 SU-8 (according to the targeted pattern sizes) was used. Standard photolithography processing was performed on an EVG 2. The last level of the mold was then developed using SU-8 developer. To anneal surface cracks and ensure good thermomechanical stability of the mold during hot embossing, a 30 – min hard baking step was performed at 180°C. For large surface devices, a silanization step using trichloro(1H,1H,2H,2H-perfluoroctyl) silane was added to facilitate demolding.

4.3 | Hot embossing and demolding

Requirements and associated criteria for the proper embossing of an SBC device can be found in Table 1. Trouble-shooting and fine-tuning of the parameters in other scenarios are noted for cases in which the corresponding requirements

were not met. The thickness and planarity of the replica were adjusted by using four screws and washers of identical length as spacers. The spacers were screwed on the tray and hot embosser temperature was set to 150 – 170°C. Once the temperature was reached, 20 min was allowed to pass to ensure a steady-state and uniform temperature inside the tray. Chunks of sTPE were aligned and stacked to reach the targeted surface and thickness on the master mold. This stack was then placed on a smooth metallic counter mold to form a ready-to-emboss stack. Before closing the tray, a Teflon sheet was used to cover up the counter-mold to avoid its adhesion to the top of the tray. The tray and oven were then closed, and vacuum pressure was applied for 60 – 180 s. The stack was then pulled out horizontally and left in a fume hood to slowly cool down to room temperature. Demolding was then performed gently using isopropanol and a flat tweezer to remove the mold and counter mold from the embossed bulk material. For recycling, discarded scraps from routine microfabrication processes were collected and kept in a closed recipient at room temperature until their use.

4.4 | Fabrication and assembly of studs

Stud interfaces were casted from melted pellets by using a metallic mold of a desired geometry following the process described in Figure 3(A). The pellets were piled in each well and the mold was heated to 215°C for 1 h in an oven. This temperature allowed the pellets to reach a sufficiently low viscosity to fill the metallic mold. The mold was was cooled down at room temperature and the demolding was carried out using a flat screwdriver and isopropanol. In 30 min, 24 smooth and bubble-free studs were obtained without applying any pressure. The studs were collected and punched through the center using a heated syringe needle, typically of gauge 18. The studs were demolded, punched, and smoothened by baking on a silicon wafer at 150 ° C for 1 min. The studs were gently pushed and remained on the wafer for 1–2 s to ensure a proper contact with the wafer. The wafer was removed and cooled down to collect the studs.

4.5 | Assessment of bonding reversibility and repeatability

Studs were bonded on a smooth SBC surface at different temperatures (room temperature, 37 ° C and 80 ° C) and time (5, 15, 30, 60, 120 min, and 72 h). A minimum of five replicates was used for each parameter. After bonding, the studs were connected using large 500 μm ID tubing to a calibrated OB1 (Elvesys, France) pressure controller connected to a 50 – ml tank containing blue food dye. The pressure was gradually increased to 10 mbar every 10 s,then to 100 mbar every 30 s until the bond burst. For reversibility tests, T-shaped channel chips were assembled with studs and baked at 80°C for 30 min. Then the chips were laid on top of a smooth sTPE substrate and left for 15 min at room temperature. PBS 1× was injected until reaching burst pressure, then the layers could be separated manually. Washing solution (isopropanol or DI water containing 0.1% SDS 15% EtOH) was used for rinsing surfaces before drying and bonding again. This process was repeated 10×.

4.6 | Experimental setup and characterization of the micromixing device

The mold structures were 100 μm thick and required 4× cycles of lithography to avoid thermal expansion during the UV exposure. The piezoelectric transducer was bonded to a $75 \times 50\,mm^2$ glass slide for 10 s using NOA and a UV lamp. Harmonic electrical signals were initiated using a function generator (AFG3011C, Tektronix, USA) with capacity of modulating signal's frequency and waveform. The function generator was then connected to an amplifier (25A250A, Amplifier Research, USA) to regulate the amplitude of the voltage and transmit the signal to the piezoelectric transducer. The electrical impedance of the transducer system was measured with an Agilent 4294A impedance analyzer (Agilent, Palo Alto, CA). A spectrum range of 10 – 100 kHz was utilized. The piezo elements were mounted on the chip and connected to low and high voltage terminals with a peak-to-peak amplitude of 1 Vpp. The highly hydrophobic surfaces of the channels were passivated by flowing a solution of bovine serum albumin (BSA) inside the channels. A PBS buffer was then used as the mobile phase to flow by an injection loop, a controlled volume of microparticles in the device.

4.7 | Epifluorescence microscopy and fluorescent particle tracking

Imaging was performed with a Nikon Eclipse epifluorescence microscope. The flow rates were controlled using a Harvard syringe pump (USA). The images were acquired using the open source microscopy software μManager 1.4.22. The videos were then analyzed using ImageJ 1.52r[53] by successively thresholding, watermarking, and particle analysis downstream to the channel using the Trackmate plugin.

4.8 | Cell culture and device perfusion

GFP+ primary mouse endothelial cells (mECs) were obtained from 6–10 weeks old GFP+ mice on a C57Bl/6 background, as described previously.[54] Cells were maintained in a 1 : 1 mixture of EGM-2 (Lonza, Canada, CC-3162) and DMEM/F12 (Wisent, QC, Canada) containing 10% FBS and 1% penicillin/streptomycin (P/S). mECs were cultured in flasks or plates coated with 0.1% gelatin (EMD Millipore ES-006-B) and used before passage 5. The microchannels were obtained using UV lithography, described in embossing protocols. The surfaces were successively hydrophilized by 100 W O_2 plasma for 10 min, coated with 0.1% gelatin (1 h at 37 ° C) and seeded for 6 h targeting a density of 10,000 cells/cm^2. The medium was removed. The chips were closed and perfused with EGM-2 at a shear stress up to 10Dyn/cm^2. After 24 – 48 h, cells were washed twice with PBS and then fixed in 4% paraformaldehyde (PFA) at room temperature in the dark for 20 min. Cells were then permeabilized in PBS + 0.1% Triton X-100 for 10 min with rocking, washed briefly with PBS, and blocked with 1% BSA in PBS for at least 1 h at room temperature. The cells were then stained with a mixture of phalloidin-iFluor594 (1/1000 in PBS) and DAPI (1/2000 in PBS) for 30 min in the dark before the final wash. Images were acquired using confocal microscopy (Zeiss LSM 780 with Zen Black 2012 software, Carl Zeiss, Germany).

ACKNOWLEDGMENTS

Maryam Tabrizian, M. Reza Rasouli, and Hugo Salmon would like to acknowledge Natural Science and Engineering Research Council of Canada (RGPIN-2016-05785) for their financial support through Discovery and Strategic Grant (STPGP 521532-18). The authors acknowledge Eden Microfluidics team for gracious material donation and constructive discussions around the Flexdym embossing. Hugo Salmon also thanks Juliette Grimaldi, Thomas Bonazzi and Sebastian Cargou from Black Hole Laboratory for their help in the burst pressure experiments.

PEER REVIEW INFORMATION

Engineering Reports thanks the anonymous reviewers for their contribution to the peer review of this work.

PEER REVIEW

The peer review history for this article is available at https://publons.com/publon/10.1002/eng2.12361.

DATA AVAILABILITY STATEMENT

The data that supports the findings of this study are available in the supplementary material of this article and from the corresponding author upon request.

CONFLICT OF INTEREST

The authors declare no financial / commercial conflict of interest.

AUTHOR CONTRIBUTIONS

Hugo Salmon: Conceptualization; data curation; formal analysis; methodology; validation; visualization; writing-original draft; writing-review and editing. **M. Reza Rasouli:** Conceptualization; data curation; formal analysis; methodology; validation; visualization; writing-original draft; writing-review and editing. **Nicholas Distasio:** Conceptualization; data curation; formal analysis; methodology; validation; writing-original draft; writing-review and editing. **Maryam Tabrizian:** Conceptualization; formal analysis; funding acquisition; investigation; methodology; project administration; visualization; writing-original draft; writing-review and editing.

ORCID

Hugo Salmon https://orcid.org/0000-0002-5486-1370
Maryam Tabrizian https://orcid.org/0000-0002-5050-4480

REFERENCES

1. Heo YS, Cabrera LM, Song JW, et al. Characterization and resolution of evaporation-mediated osmolality shifts that constrain microfluidic cell culture in poly(dimethylsiloxane) devices. *Anal Chem*. 2007;79:1126-1134.
2. Toepke MW, Beebe DJ. PDMS absorption of small molecules and consequences in microfluidic applications. *Lab Chip*. 2006;6:1484-1486.
3. Regehr KJ, Domenech M, Koepsel JT, et al. Biological implications of polydimethylsiloxane-based microfluidic cell culture. *Lab Chip*. 2009;9:2132-2139.
4. Eddington DT, Puccinelli JP, Beebe DJ. Thermal aging and reduced hydrophobic recovery of polydimethylsiloxane. *Sens Actuators B*. 2006;114:170-172.
5. Serra M, Pereiro I, Yamada A, Viovy J-L, Descroix S, Ferraro D. A simple and low-cost Chip bonding solution for high pressure, high temperature and biological applications. *Lab Chip*. 2017;17:629-634.
6. Vittayarukskul K, Lee AP. A truly Lego ® -like modular microfluidics platform. *J Micromech Microeng*. 2017;27:035004.
7. Fan Y, Liu S, He J, Gao K, Zhang Y. Rapid prototyping of flexible multilayer microfluidic devices using polyester sealing film. *Microsyst Technol*. 2018;24:2847-2852.
8. Pitingolo G, Riaud A, Nastruzzi C, Taly V. Tunable and reversible gelatin-based bonding for microfluidic cell culture. *Adv Eng Mater*. 2019;21:1900145.
9. Perrault CM, Salmon H, Mercier O, Roy E. Insights on polymers for microfluidics applied to biomedical applications. *Res Rev Polym*. 2017;8:106.
10. Roy E, Galas J-C, Veres T. Thermoplastic elastomers for microfluidics: towards a high-throughput fabrication method of multilayered microfluidic devices. *Lab Chip*. 2011;11:3193-3196.
11. Bruijns B, Veciana A, Tiggelaar R, Gardeniers H. Cyclic olefin copolymer microfluidic devices for forensic applications. *Biosensors*. 2019;9:85.
12. Geissler M, Roy E, Diaz-Quijada GA, Galas J-C, Veres T. Microfluidic patterning of miniaturized DNA arrays on plastic substrates. *ACS Appl Mater Interfaces*. 2009;1:1387-1395.
13. Miserere S, Mottet G, Taniga V, Descroix S, Viovy J-L, Malaquin L. Fabrication of thermoplastics chips through lamination based techniques. *Lab Chip*. 2012;12:1849-1856.
14. Perez-Toralla K, Champ J, Reza Mohamadi M, et al. New non-covalent strategies for stable surface treatment of thermoplastic chips. *Lab Chip*. 2013;13:4409-4418.
15. Xue B, Geng Y, Yan Y, Ma G, Wang D, He Y. Rapid prototyping of microfluidic Chip with Burr-free PMMA microchannel fabricated by revolving tip-based micro-cutting. *J Mater Process Technol*. 2020;277:116468.
16. Leech PW. Hot embossing of cyclic olefin copolymers. *J Micromech Microeng*. 2009;19:055008.
17. Shiu PP, Knopf GK, Ostojic M, Nikumb S. Rapid fabrication of tooling for microfluidic devices via laser micromachining and hot embossing. *J Micromech Microeng*. 2008;18:025012.
18. Attia UM, Marson S, Alcock JR. Micro-injection Moulding of polymer microfluidic devices. *Microfluid Nanofluid*. 2009;7(1):1-28.
19. Lachaux J, Alcaine C, Gomez-Escoda B, et al. Thermoplastic elastomer with advanced Hydrophilization and bonding performances for rapid (30 s) and easy molding of microfluidic devices. *Lab Chip*. 2017;17:2581-2594.
20. Roy E, Geissler M, Galas J-C, Veres T. Prototyping of microfluidic systems using a commercial thermoplastic elastomer. *Microfluid Nanofluidics*. 2011;11:235-244.
21. Holden G, ed. *Thermoplastic Elastomers*. Munich, New York, Cincinnati: Hanser Publishers; Hanser/Gardner Publications; 1996.
22. Guillemette MD, Roy E, Auger FA, Veres T. Rapid isothermal substrate microfabrication of a biocompatible thermoplastic elastomer for cellular contact guidance. *Acta Biomater*. 2011;7:2492-2498.
23. Berthier E, Young EWK, Beebe D. Engineers are from PDMS-land, biologists are from Polystyrenia. *Lab Chip*. 2012;12:1224-1237.
24. Yu J, Berthier E, Craig A, et al. Reconfigurable open microfluidics for studying the spatiotemporal dynamics of paracrine signalling. *Nat Biomed Eng*. 2019;3:830-841.
25. Mukhopadhyay R. When PDMS Isn't the best. *Anal Chem*. 2007;79:3248-3253.
26. Pivetal J, Pereira FM, Barbosa AI, Castanheira AP, Reis NM, Edwards AD. Covalent immobilisation of antibodies in Teflon-FEP microfluidic devices for the sensitive quantification of clinically relevant protein biomarkers. *Analyst*. 2017;142:959-968.
27. Zhou XC, Sjöberg R, Druet A, et al. Thiol–Ene–epoxy thermoset for low-temperature bonding to biofunctionalized microarray surfaces. *Lab Chip*. 2017;17:3672-3681.
28. Shaegh SAM, Pourmand A, Nabavinia M, et al. Rapid prototyping of whole-thermoplastic microfluidics with built-in microvalves using laser ablation and thermal fusion bonding. *Sens Actuators B*. 2018;255:100-109.
29. Aboud N, Ferraro D, Taverna M, Descroix S, Smadja C, Tran NT. Dyneon THV, a fluorinated thermoplastic as a novel material for microchip capillary electrophoresis. *Analyst*. 2016;141:5776-5783.
30. Lachaux J, Salmon H, Loisel F, et al. Soft thermoplastic elastomer for easy and rapid spin-coating fabrication of microfluidic devices with high Hydrophilization and bonding performances. *Adv Mater Technol*. 2019;4:1800308.

31. Pasman T, Grijpma D, Stamatialis D, Poot A. Flat and microstructured polymeric membranes in organs-on-chips. *J Royal Soc Interf*. 2018;15:20180351.
32. Nelson MD, Ramkumar N, Gale BK. Flexible, transparent, sub-100 $\mathrm\m U$m microfluidic channels with fused deposition modeling 3D-printed thermoplastic polyurethane. *J Micromech Microeng*. 2019;29:095010.
33. Nguyen H-T, Thach H, Roy E, Huynh K, Perrault C. Low-cost, accessible fabrication methods for microfluidics research in low-resource settings. *Micromachines*. 2018;9:461.
34. Drobny JG. *Handbook of Thermoplastic Elastomers*. Amsterdam, Netherlands: Elsevier; 2014.
35. Worgull M. Hot embossing process. In: Worgull M, ed. *Hot Embossing*. Boston: William Andrew Publishing; 2009:137-177.
36. Temiz Y, Lovchik RD, Kaigala GV, Delamarche E. Lab-on-a-Chip devices: how to close and plug the lab? *Microelectron Eng*. 2015;132:156-175.
37. Dekker S, Buesink W, Blom M, et al. Standardized and modular microfluidic platform for fast lab on Chip system development. *Sens Actuators B*. 2018;272:468-478.
38. Gossett DR, Weaver WM, Mach AJ, et al. Label-free cell separation and sorting in microfluidic systems. *Anal Bioanal Chem*. 2010;397:3249-3267.
39. Huh D, Kim HJ, Fraser JP, et al. Microfabrication of human organs-on-chips. *Nat Protoc*. 2013;8:2135-2157.
40. Mannino RG, Myers DR, Ahn B, et al. Do-it-yourself in vitro vasculature that recapitulates in vivo geometries for investigating endothelial-blood cell interactions. *Sci Rep*. 2015;5:12401. https://doi.org/10.1038/srep12401.
41. Sfriso R, Zhang S, Bichsel CA, et al. 3D artificial round section micro-vessels to investigate endothelial cells under physiological flow conditions. *Sci Rep*. 2018;8:5898. https://doi.org/10.1038/s41598-018-24273-7.
42. Rasouli MR, Tabrizian M. An ultra-rapid acoustic micromixer for synthesis of organic nanoparticles. *Lab Chip*. 2019;19:3316-3325.
43. Saha B, Toh WQ, Liu E, Tor SB, Hardt DE, Lee J. A review on the importance of surface coating of micro/Nano-Mold in micro/Nano-molding processes. *J Micromech Microeng*. 2015;26:013002.
44. Zhang Y-L, Xia H, Kim E, Sun H-B. Recent developments in Superhydrophobic surfaces with unique structural and functional properties. *Soft Matter*. 2012;8:11217.
45. Malic L, Daoud J, Geissler M, et al. Epigenetic subtyping of white blood cells using a thermoplastic elastomer-based microfluidic emulsification device for multiplexed, methylation-specific digital droplet PCR. *Analyst*. 2019;144:6541-6553.
46. Drobny JG. Styrenic block copolymers. In: Drobny JG, ed. *Handbook of Thermoplastic Elastomers*. Norwich, NY: William Andrew Publishing; 2007:161-177.
47. Creton C. Block copolymers for adhesive applications. *Macromolecular Engineering*. Hoboken: Wiley-Blackwell; 2011:1731-1751.
48. Armani D, Liu C, Aluru N. Technical digest. Paper presented at: Proceedings of the IEEE International MEMS 99 Conference. 12th IEEE International Conference on Micro Electro Mechanical Systems (Cat. No.99CH36291), Orlando, FL, USA; 1999:222-227; IEEE.
49. Liu M, Sun J, Sun Y, Bock C, Chen Q. Thickness-dependent mechanical properties of polydimethylsiloxane membranes. *J Micromech Microeng*. 2009;19:035028.
50. Langer K, Bremond N, Boitard L, Baudry J, Bibette J. Micropipette-powered droplet based microfluidics. *Biomicrofluidics*. 2018;12:044106.
51. Ahmed D, Mao X, Juluri BK, Huang TJ. A fast microfluidic mixer based on acoustically driven sidewall-trapped microbubbles. *Microfluid Nanofluid*. 2009;7:727-731.
52. Garg R, Qadri A. Hemoglobin transforms anti-inflammatory salmonella typhi virulence polysaccharide into a TLR-2 agonist. *J Immunol*. 2010;184:5980-5987.
53. Schneider CA, Rasband WS, Eliceiri KW. NIH image to ImageJ: 25 years of image analysis. *Nat Methods*. 2012;9:671-675.
54. DiStasio N, Arts M, Lehoux S, Tabrizian M. IL-10 gene transfection in primary endothelial cells via linear and branched poly(β-amino Ester) nanoparticles attenuates inflammation in stimulated macrophages. *ACS Appl Bio Mater*. 2018;1:917-927.

SUPPORTING INFORMATION

Additional supporting information may be found online in the Supporting Information section at the end of this article.

How to cite this article: Salmon H, Rasouli MR, Distasio N, Tabrizian M. Facile engineering and interfacing of styrenic block copolymers devices for low-cost, multipurpose microfluidic applications. *Engineering Reports*. 2021;e12361. https://doi.org/10.1002/eng2.12361